Published in final edited form as:
Mol Cell Neurosci. 2012 August ; 51(1-2): 43–52. doi:10.1016/j.mcn.2012.07.009.

Amyloid precursor protein (APP) regulates synaptic structure and function

Sheue-Houy Tyan[a], **Ann Yu-Jung Shih**[a,c], **Jessica J. Walsh**[b], **Hiroko Murayama**[a], **Floyd Sarsoza**[a], **Lawrence Ku**[a], **Simone Eggert**[a,d], **Patrick R. Hof**[b], **Edward H. Koo**[a], and **Dara L. Dickstein**[b]

[a]Department of Neurosciences, University of California San Diego, La Jolla, CA, USA

[b]Fishberg Department of Neuroscience and Friedman Brain Institute, Mount Sinai School of Medicine, New York, NY, USA

Abstract

The amyloid precursor protein (APP) plays a critical role in Alzheimer's disease (AD) pathogenesis. APP is proteolytically cleaved by β- and γ-secretases to generate the amyloid β-protein (Aβ), the core protein component of senile plaques in AD. It is also cleaved by α-secretase to release the large soluble APP (sAPP) luminal domain that has been shown to exhibit trophic properties. Increasing evidence points to the development of synaptic deficits and dendritic spine loss prior to deposition of amyloid in transgenic mouse models that overexpress APP and Aβ peptides. The consequence of loss of APP, however, is unsettled. In this study, we investigated whether APP itself plays a role in regulating synaptic structure and function using an APP knock-out (APP−/−) mouse model. We examined dendritic spines in primary cultures of hippocampal neurons and CA1 neurons of hippocampus from APP−/− mice. In the cultured neurons, there was a significant decrease (~35%) in spine density in neurons derived from APP−/− mice compared to littermate control neurons that were partially restored with sAPPα-conditioned medium. In APP−/− mice *in vivo*, spine numbers were also significantly reduced but by a smaller magnitude (~15%). Furthermore, apical dendritic length and dendritic arborization were markedly diminished in hippocampal neurons. These abnormalities in neuronal morphology were accompanied by reduction in long-term potentiation. Strikingly, all these changes *in vivo* were only seen in mice that were 12-15 months in age but not in younger animals. We propose that APP, specifically sAPP, is necessary for the maintenance of dendritic integrity in the hippocampus in an age-

Address for correspondence to: Sheue-Houy Tyan, Department of Neurosciences, University of California San Diego, 9500 Gilman Drive, La Jolla CA 92093. USA. s1tyan@ucsd.edu Dara L. Dickstein, Department of Neurosciences Mount Sinai School of Medicine, 1425 Madison Avenue, New York NY, 10029, USA. dara.dickstein@mssm.edu.
[c]Current Address: ActivX Biosciences, La Jolla, CA, USA
[d]Current Address: Department of Human Biology and Human Genetics, Technical University of Kaiserslautern, Kaiserslautern, Germany

Competing interests The authors declare that they have no competing interests.

Author's contributions SHT designed, performed the experiments and wrote the manuscript. AS and FS performed laser scanning microscope on *in vivo* spine images. JW performed cell tracing and analyzing dendritic morphology for *in vivo* studies. HM performed the Western blot analysis. LK contributed to data analysis on *in vivo* studies. SE provided the APP-deficient mice. DLD designed and conducted the *in vivo* dendritic morphology studies and contributed to write the manuscript. PRH provided critical input to the *in vivo* dendritic morphology studies and to the manuscript. EK critically discussed experimental design and wrote the manuscripts with SHT and DLD. All authors have read and approved the final manuscript.

associated manner. Finally, these age-related changes may contribute to Alzheimer's changes independent of Aβ-mediated synaptic toxicity.

Keywords

Alzheimer's disease; amyloid precursor protein; knock-out mice; extracellular domain; soluble amyloid β; synapse

Introduction

The amyloid precursor protein (APP) is considered to play a central role in the pathogenesis of Alzheimer's disease (AD). APP is the precursor of amyloid β-protein (Aβ), the main component of amyloid plaques, and as such has given rise to the amyloid cascade hypothesis for AD, which posits that the misprocessing and abnormal regulation of APP leads to the gradual overproduction or accumulation of Aβ into oligomers and extracellular plaques, initiating a sequence of events that results in AD (Hardy and Selkoe, 2002). APP is a type I transmembrane protein with a large N-terminal extracellular domain and a short cytoplasmic domain. APP undergoes multiple proteolytic steps: cleavage by either α- or β-secretase releases the large APP ectodomain, sAPPα and sAPPβ respectively; leaving the membrane-anchored C-terminal fragments (CTFs) (Sisodia et al., 1993; Turner et al., 2003). The CTFs can be further cleaved by γ-secretase to generate Aβ peptides, while releasing the APP intracellular domain (AICD), which is thought to contribute to cell signaling or cell death (Konietzko, 2011).

In addition to being the precursor to Aβ, a number of physiological functions have been attributed to APP, including, but not limited to, synapse formation, neuronal survival, and neuritic outgrowth (De Strooper and Annaert, 2000; Mattson, 1995, 1997; Nunan et al., 2001; Russo et al., 1998; Turner et al., 2003). APP belongs to a highly conserved gene family including the amyloid precursor-like proteins, APLP1 and APLP2 (Anliker and Muller, 2006). It is encoded on chromosome 21 and is alternatively spliced into 3 main isoforms, APP695, APP751, and APP770. Individuals with Down syndrome (trisomy 21) or inherited cases of familial AD with point mutations in the APP gene invariably develop AD pathology (Epstein, 1990; Potter, 1991). This link of APP to AD pathology and the many putative functions of APP in neurons led to the establishment of many invertebrate and transgenic mouse models, both knock-in (4 with truncated alleles and 2 with C-terminal point mutation alleles) and knock-out (2 KO and 2 conditional), that suffer from various defects and abnormalities (reviewed in (Guo et al., 2011). One APP KO mouse generated by Zheng et al. (1995) shows many deficits in locomotor activity and forelimb grip strength, as well as impairments in learning and memory associated with deficits in long-term potentiation (LTP) (Ring et al., 2007). In fact alterations in synaptic structure and function are some of the most consistent findings of *in vitro* studies using neurons from either APP-deficient mice or from RNAi-mediated knockdown approaches (Herard et al., 2006; Hoe et al., 2009; Lee et al., 2010; Seabrook et al., 1999; Zheng et al., 1995). This APP mouse model also shows changes in dendritic arborization (Seabrook et al., 1999) and synapse numbers (Lee et al., 2010), although the latter finding was not supported by another study (Phinney et al., 1999). In contrast, a study using autaptic hippocampal cultures derived from a different APP KO mouse line showed an increase in synaptophysin-immunoreactive puncta and miniature synaptic currents (Priller et al., 2006). These conflicting results are compounded by APLP1 and APLP2, which likely play redundant functions that compensate for the loss of APP in the intact animal. However, more recent studies in double APP/APLP2-deficient, but not single APP KO, animals have clearly identified developmental

defects in neuromuscular junction synapses with corresponding neurophysiological deficits (Wang et al., 2005). Thus, the situation with single APP KO mice remains unresolved.

Until recently, the conventional methods to investigate structure of synaptic and dendritic morphology have been Golgi staining, immunostaining of synaptic proteins, imaging by fluorescent markers such as GFP labeling, or by ultrastructure. These techniques, however, infer, but do not directly assay, number of synapses and underestimate the number of dendritic spines (Friedland et al., 2006; Pilati et al., 2008). To provide convincing evidence that APP is required for the maintenance of dendritic structure, synapse formation, and synaptic function, we re-examined the effect of APP on synaptic plasticity and dendritic and spine morphology in an APP KO mouse line using 3-dimensional reconstruction of individual neurons and spines to analyze accurately alterations in dendritic and spine structure *in vivo*. We also conducted *in vitro* studies in neurons from APP KO mice to assess whether spine density differences were accompanied by alterations in synaptic plasticity or basal synaptic transmission.

Results

APP deficiency decrease spine number and dendritic branching in primary hippocampal neurons

We re-examined the potential role of APP in synaptic function by focusing on dendritic spines in APP−/− neurons by both *in vitro* and *in vivo* approaches. First, we measured dendritic spine densities from hippocampal neurons cultured from P0-P1 neonatal pups from APP+/+, APP+/−, and APP−/− mice (Fig. 1A, B). The spine density in APP−/− neurons was significantly decreased by almost 40% compared to APP+/+ (36.8%, $p < 0.001$, one-way ANOVA with Tukey's post-hoc test) and APP+/− (35%, $p < 0.001$). In this analysis, 45 neurons were scored from a total of 11 APP+/+ mice, 64 neurons from 15 APP+/− mice, and 85 neurons from 21 APP−/− mice. Thus, APP−/− primary hippocampal neurons in culture showed a markedly diminished dendritic spine number as a measure of synaptic density. There was, however, no appreciable difference between wild type and hemizygous APP-deficient neurons. Therefore, to simplify subsequent breeding for *in vivo* analyses, we have chosen to focus our comparison primarily between APP+/− and APP−/− mice. We also noticed a reduction of dendritic complexity in culture hippocampal neurons from APP deficient mice. However, in cultured neurons, it is difficult to precisely define the apical vs. basal dendrites to quantify such changes in neuronal polarity. Therefore, the number of dendritic branch points within a radius of 150 μm from the neuron soma was assayed as a measure of dendritic complexity. We found that the average number of dendritic branch points was significantly reduced in APP−/− neurons compared to APP+/− (Fig. S3), indicating that both dendritic spine numbers and dendritic arborizations were diminished in the absence of APP in cultured hippocampal neurons.

Dendritic and spine morphology in APP knock-out mice

The marked reduction in dendritic spine numbers in cultured hippocampal neurons from APP−/− mice was surprising as this alteration has, to our knowledge, not been reported before. In fact, autaptic neurons from APP−/− mice showed an increase in synaptophysin-immunopositive puncta (Priller et al., 2006). We also observed a decrease in dendritic branching in APP−/− neurons in primary cultures (Fig. 1). Thus, we next evaluated the dendritic and spine morphology in APP−/− mice *in vivo* in more detail. Brain slices of five to six animals in each group (APP+/− and APP−/−) from two ages were examined (2-4 months-old and 12-15 months-old). We first examined each Lucifer Yellow-injected neuron for various morphometric parameters (i.e. dendritic length and complexity) by performing 3-dimensional tracing of each neuron. Sholl analyses showed that CA1 neurons in old APP−/−

mice (~13 months old) are significantly less complex in apical arbors than in control (APP+/−) mice (Fig. 2A, B). Apical dendritic length was also shorter in old APP−/− mice compared to APP+/− mice, but no significant changes were seen in basal dendritic length (Table 1). Further analysis showed that CA1 neurons from old APP−/− mice showed significantly shorter apical lengths, specifically between 60 and 180 μm away from the soma (overall interaction $F(11,110) = 1.76$, $p = 0.07$; effect of genotype $F(1, 10) = 5.21$, $p = 0.04$, distance from soma $F(11,110) = 79.46$, $p < 0.0001$; Fig. S1A). Significant differences in Sholl analysis of basal dendritic length and number of intersections were also seen (overall interaction for Sholl and number of interaction respectively $F(7,70) = 2.235$, $p = 0.003$; $F(7,70) = 2.78$, $p = 0.01$; Fig. S1B). In contrast, young APP−/− animals (2-4 months old) did not show a reduction in the complexity of apical dendrites. Not surprisingly, there were no changes in both apical and basal dendritic length in young mice (Fig. 2E and F and Table 1). In addition, we examined whether there was an age-dependent reduction in dendritic length in control mice and found that CA1 neurons exhibited similar apical and basal dendritic lengths between the young and old animals (Table 1). However, old APP−/− mice showed significantly shorter apical but not basal dendritic length compared to the young APP−/− mice ($p = 0.01$, unpaired *t*-test; Table 1).

We next quantified dendritic spine density from apical dendrites in the microinjected neurons in CA1 (Fig. 3A) because our previous analysis detected morphological changes in apical dendrites only. Spine number was decreased by a small but significant 15% in old APP−/− mice compared to old APP+/− mice (Fig. 3B). In young mice, however, there was no reduction in spine density in young APP−/− compared to young APP+/− mice (Fig. 3B). In young mice, however, there was a non-significant trend in reduction in spine density in young APP−/− compared to young APP+/− mice (Fig. 3B, $p > 0.05$). Further analyses showed no changes in three types of dendritic spines (thin, stubby, and mushroom) classified using the Rayburst-based shape analysis algorithm (Rodriguez et al., 2006). Thus, the reduction in dendritic spine density in old APP−/− mice apparently extended through all spine subtypes (Fig. S2 and Table 1). There was also no difference in mean spine volume for all spines and subtypes in old APP−/− mice compared to controls. However, we did find a significant difference in spine volume in old APP−/− mice compared to young mice ($p = 0.02$, old APP−/− *vs.* young APP−/−).

Loss of APP leads to impaired synaptic function in old APP knock-out mice

To investigate whether the spine loss in APP−/− mice is correlated with impairment in synaptic function, we examined LTP, basal synaptic transmission, and the paired-pulse facilitation in both old (~13 months old) and young (2-4 months old) animals. LTP was measured after tetanic stimulation by four trains of 1-s 100 Hz stimulations. We saw a marked impairment in LTP in old APP−/− mice as compared to controls but not in young APP−/− (Fig. 4A, B). The slope of fEPSP in the old APP +/− was 296.47 ± 6.07% compared to 134.83 ± 4.52% in the APP−/− mice 60 minutes after LTP induction (Fig. 4A). Consistent with the *in vivo* morphological studies, there was no impairment in LTP in young APP KO mice as seen in the old animals (Fig. 4B). The basal transmissions were examined by plotting the input-output (I-O) curve (fiber volley against fEPSP slope). There was no difference in input/output ratio of APP+/− *vs.* APP−/− at either age group (Fig. 4C, D). Thus the reduction in LTP was not mirrored by changes in basal synaptic transmission. Finally, paired-pulse facilitation was similar between APP−/− and control mice in both age groups (Fig. 4E, F) indicating no presynaptic impairment in the hippocampus of APP−/− mice.

Mechanisms contributing to deficits in spine numbers in APP knock-out hippocampal neurons

Having established that APP deficiency results in reduced dendritic spine numbers both *in vitro* and *in vivo*, we next sought to establish whether this is a consequence of a lack of sAPP, which is shed following α- or β-secretase cleavage. A number of studies have shown that sAPPα exhibits neurotrophic properties (Ring et al., 2007; Weyer et al., 2011; Zheng and Koo, 2011) but whether the primary function of APP requires the transmembrane or cytoplasmic domain is debated (Barbagallo et al., 2011; Lee et al., 2010; Li et al., 2010). To test whether lack of sAPP is responsible for spine loss in APP−/− neurons in culture, conditioned medium from wild type neurons (APP WT-CM) was added to APP−/− primary hippocampal neurons starting at DIV 2 (with repeated addition every other day). As before, the neurons were transfected with eGFP at DIV 16-21 and spine density was assessed. In cultures with wild type neuron conditioned medium, the deficit in spine density seen in APP −/− neurons was essentially restored to normal levels (Fig. 5). In addition, the number of branch points in APP−/− neurons was also restored by adding APP WT-CM (Fig. S3, APP WT-CM: 28.4 ± 1.0; APP+/−: 29.7 ± 1.6; APP−/−: 17.1 ± 1.0; $p < 0.001$, one-way ANOVA with Tukey's post-hoc test). This indicated that molecules, absent in APP−/− mice, and constitutively secreted from normal neurons, are necessary to induce or maintain a normal level of dendritic spine, and likely synapse, numbers. A possible candidate is obviously sAPP. To test this hypothesis, we generated stable cell lines in mouse B103 cells that express full-length mouse APP or only sAPPα or sAPPβ by introducing a stop codon at the α- or β-secretase site, respectively, to truncate APP at the C-terminal (Fig. 6A & B). B103 cells were chosen because they lack endogenous mouse APP (Schubert and Behl, 1993). As expected, western blot analyses of the various transfected cell lines confirmed the presence of sAPP in culture media but these constructs lack the C-terminus when immunoblotted in cell lysates, the latter using an antibody specific to the C-terminus (Fig. 6B). By dot blot assay, we estimated that the stably transfected cells expressed approximately 20-fold higher sAPP in conditioned medium than wild type neurons (data not shown). After adjusting for the level of sAPP (20x dilution with neurobasal medium), conditioned medium from sAPPα- or sAPPβ-transfected B103 cells was applied to hippocampal neurons derived from either APP wild type or APP−/− mice at DIV 2. We found the spine numbers were significantly but only partially restored by sAPPα-B103 CM (Fig. 6C). Similar to dendritic spine numbers, the number of dendritic branch points were also significantly but only partially restored by sAPPα-B103 CM (Fig. S3). On the other hand, the sAPPβ-CM did not have any effects on spine number in APP−/− neurons (Fig. 6C), confirming the notion that a major domain of the sAPP trophic property reside within the 17 amino acid region at the C-terminus of sAPPα.

However, we noted a trend in reduction in spine density following B103-CM treatment alone. At lower dilutions of conditioned medium, i.e. more concentrated, the cultured neurons were distinctly unhealthy (data not shown). Therefore, the degree of rescue in the sAPPα-B103 medium may have been artefactually depressed due to the experimental paradigm of using B103 cells. Nonetheless, the results strongly suggested that lack of sAPPα is a major factor accounting for spine loss in APP−/− neurons.

Discussion

Establishing the physiological function of APP *in vivo* has been difficult, in part because of likely redundant functions of APLP1 and APLP2 and in part because some of the previous approaches used to assess synaptic structure may have been insensitive to small changes. In this study, we combined neuronal cell filling with Lucifer Yellow coupled with a sensitive, quantitative, and 3-dimensional, automated system to examine dendritic spine numbers and dendritic morphology *in vivo* in APP−/− mice. Further, electrophysiology from acute

hippocampal slices and *in vitro* analyses of cultured primary hippocampal neurons were performed to complement these studies. Unexpectedly, we observed that dendritic spine densities were significantly reduced in cultured primary hippocampal neurons deficient in APP and this was confirmed in apical dendrites of CA1 hippocampal neurons *in vivo*, albeit to a much lesser extent. Importantly, the reduction in spines and marked reduction in dendritic length and branching were seen only in older (12-14 months) but not in young (2-4 months) APP−/− animals. Furthermore, consistent with changes in altered neuronal morphology in older animals, synaptic plasticity as measured by LTP was also impaired only in older but not young APP−/− mice, the former in agreement with previous reports. The marked reduction dendritic spine densities *in vitro* in APP−/− neurons and the restoration of this loss by conditioned medium from wild type neurons suggests that secreted sAPP, in particular sAPPα rather than sAPPβ, plays an important in maintaining spines. Taken together, these results indicate that deficiency in APP alone results in gradual reduction in dendritic structure and synaptic function during aging. This suggests a physiological role of APP in the maintenance rather than in the formation of dendritic spine structure.

In cultured hippocampal neurons, we found a ~35% decrease in spine number in APP−/− mice which was confirmed in CA1 neurons in 12-15 months old APP−/− mice but to a much lesser degree. Several reasons may account for this difference. A first, rather simple, explanation may be that heterozygous APP mice only carry one copy of APP, and as such there is only ~15% decrease in APP−/− mice compared to APP+/− mice. However, because we did not find such dose-response in cultured neurons, we focused on heterozygous instead of wild type animals in the *in vivo* studies to simplify both the breeding and analyses. Nevertheless, it is reassuring that both the *in vitro* and *in vivo* studies demonstrated similar reductions in dendritic spine density, thus providing further confidence that absence of APP has deleterious effects on dendritic spines in an age-related manner. The second possibility is the fact that the brain environment is imperfectly modeled in a culture system that lacks the normal complement of different cell types, such glial cells. Furthermore, the neuronal connectivity is also decreased in *in vitro* cultures compared to the brain *in vivo*.

It is important to note that some studies showed no synaptic bouton loss (Phinney et al., 1999), normal neurite outgrowth (Harper et al., 1998) and a near two-fold increase in spine density in APP deficient neurons (Bittner et al., 2009). The reason for these inconsistent results is unclear but may be due to the different APP−/− mice lines, strain background, and types of neuron that were assessed, and the methods used for quantifying the spines (both *in vitro* and *in vivo*). Here, we complemented the studies in cultured hippocampal neurons from APP−/− mice with appropriate rescue experiments. Further, in both *in vitro* and *in vivo* experiments, we directly measured dendritic spines rather than using surrogate measurements, such as synaptophysin immunostaining. More specifically, we cultured hippocampal neurons from APP−/− mice instead of RNAi knockdown, which may not deplete APP completely, and scored actual spine numbers rather than immunostained for synaptic markers. In addition, we used mouse instead of human APP to generate sAPP to validate the importance of sAPPα on synaptic morphology. Furthermore, we did not observe such rescue effects on spine number from sAPPβ conditioned medium. The different effects on spine number between sAPPα and β are intriguing as this supports the concept that a trophic domain is encoded in the 17 amino acids at the C-terminus of sAPPα that is lacking in sAPPβ (Mattson, 1997). Finally, we used a new 3-dimensional imaging technique to study dendrite and spine morphology more precisely and also systematically analyzed the spine volume and spine types in young and old APP−/− mice. This analysis has been shown to be much more accurate than the use of Golgi staining which is restricted in the level of resolution of the spines analyzed, as well as by the fact that spine number in Golgi preparations can only be reliably assessed in the x-y plane and omits the spines in the z-

plane, thus resulting in a significant underestimation of spine density (Duan et al., 2003). Nevertheless, the results of our study support the hypothesis that APP is crucial for maintaining dendritic morphology and spine structures as well as synaptic plasticity.

An important finding from the *in vivo* studies was that the changes in neuronal morphology in the older group of APP-deficient mice were absent in the young mice. We did not anticipate these age-associated alterations given the observations from cultured hippocampal neurons (Fig. 1). Specifically, the reduction in apical dendritic length, dendritic arborization, and spine density were only present in the older cohort of animals (Table 1). Our findings therefore suggest that APP plays a specific role in the maintenance of dendritic complexity and spine numbers that manifest itself during the aging process. The number of dendritic spines is generally believed to be an end result of a balance between spine formation and spine elimination. Because spine density was unchanged in the younger animals and because addition of new stable dendritic spines is thought to be infrequent in adult mice (Alvarez and Sabatini, 2007), we hypothesize that the reduction in spine density in the older animals is the result of increased spine elimination. In this context, it is noteworthy that the reduction in dendritic complexity is of greater magnitude than the small but significant reduction in spine density. Whether all of these changes are due to the putative trophic properties of APP, or the lack thereof, is unclear. In a previous report, disruption of immunostaining for the postsynaptic marker MAP-2 and the presynaptic marker synaptophysin had been observed. However, there was no detectable decrease in these protein levels at 12 month of age in APP −/− mice (Seabrook et al., 1999), which is probably due to only a minimal reduction of spine number. Not surprisingly, PSD-95 and synaptophysin levels by Western blotting were not reduced in APP−/− brains as compared to wild type mice (Fig. S4). More interesting is why these changes were only evident when the mice were aged. Perhaps the compensatory effects of APLP1 and APLP2 diminish with age, an explanation frequently invoked when the mild phenotype of the APP-deficient mice was first described. Although no compensatory changes in APLP1 or APLP2 expression were detected in 14 weeks old APP −/− mice (Zheng et al., 1995), it is not clear whether there is a reduction in expression of the APP orthologs with age. In this regard, a parallel study in APLP2 failed to detect any changes in dendritic morphology or spine density in either young or old animals (Midthune et al., 2012), a situation that is quite different from what we saw in the present study. Consequently, it will be interesting to determine whether there is an age-associated reduction in the expression or levels of APLP1 or APLP2.

The most consistent finding of neuronal function of APP is perhaps its role as a neurotrophic factor and in synaptogenesis, a neuronal function potentially related to its cell adhesion activity. APP has been shown to be localized to the tips of growing nerve fibers while changes in APP processing from full-length to sAPP have also been shown to be tightly regulated in this process, implicating APP in synapse formation (Moya et al., 1994). The obvious explanation for the mechanism of abnormal dendritic morphology developing in APP−/− mice is the concomitant loss of APPs secretion in the absence of APP in primary cultures, the fact that the reduction in dendritic spines can be restored simply by culturing the APP-deficient neurons in media conditioned from wild type neurons implied that the loss of soluble factors are causative of these alterations. Furthermore, we observed partial restoration of dendritic spine numbers in APP-deficient neurons after the addition of media from N2a cells transfected with mouse α-secretase cleaved sAPPα (Fig. 6). As described, the restoration was incomplete but this could be due to incompatibility of media conditioned by N2a cells because we saw a reduction in dendritic spine numbers in neurons cultured with mock transfected media (data not shown). On the other hand, recent studies using APP knock-in mice to rescue the postnatal lethality of APP-APLP2 double knock-out mice suggested that knock-in mice expressing only sAPPα, i.e. truncated after the α-secretase site identical to our sAPPα construct, are hypomorphic with respect to APP function (Weyer et

al., 2011). Specifically, in the setting of APLP2 deficiency, sAPPα knock-in mice which survive into adulthood demonstrated abnormal hippocampal and neuromuscular functions. These observations imply that the transmembrane and/or intracellular domains of APP carry out additional essential physiological functions. Consequently, our results are highly suggestive of sAPPα playing a major but not exclusive role in these dendritic defects. Given the findings of the APP-APLP2 deficient mice, it is highly likely that the C-terminus of APP also contribute to normal APP function, an interesting possibility that was not addressed in this study. In addition, our results are quite consistent with other reports describing the reduction in dendritic spine numbers following RNAi-mediated knockdown of APP or after deletion of the E1 and E2 domains of APP, the latter being located in the extracellular region contained within APPs (Lee et al., 2010). However, the precise mechanisms by which APPs functions as a trophic molecule in a paracrine fashion have not been elucidated yet. Lastly, the fact that a *bona fide* receptor for APPs has not been established adds to the difficulty in understanding how APP is mediating these effects.

In conclusion, our data defines a role of APP in maintenance of dendritic structure and synapse formation and function. We demonstrated that the loss of APP results in alterations in dendritic length and complexity, and spine density in old APP−/− mice and in cultured hippocampal neurons. These changes were correlated with impairment in synaptic function as indicated by the decrease in LTP. Importantly, our data suggests that this physiological role of APP is age-dependent, seen only in aged animals. While the complete cellular functions of full-length APP and its proteolytic cleavage fragments are still incompletely characterized, it is possible that their role in synapse maintenance may, in part, underlie the cognitive deficits and neuronal pathology observed in AD.

Materials and methods

Animals

APP−/− mice were kindly provided by Dr. Hui Zheng (Zheng et al., 1995) and were backcrossed to C57BL/6 for more than 10 generations. The mice were kept as heterozyqous (APP+/−) or homozygous knock-out (APP−/−) background. All animal procedures were approved by the Institutional Animal Care and Use Committee at UCSD, and in accordance with the National Institutes of Health guidelines.

Hippocampal culture and transfection

Primary hippocampal neurons were cultured from P0 to P1 pups from APP+/− bred to either APP+/− or APP−/− to obtain the desired genotypes. Individual hippocampi from each pup were dissected and processed separately. Genotyping by PCR was performed from a sample of the tail from each pup. Following genotyping, hippocampal cultures remained separate regardless of the genotype (APP+/+, APP+/−, or APP−/−) and were analyzed separately. The hippocampal cultures were prepared at a density of 300 cells/mm^2 on poly-L-lysine-coated coverslips and maintained in neurobasal medium with B-27 supplement (Calabrese et al., 2007). The neurons were transfected with pEGFP-N3 plasmid to visualize dendritic spines (Clontech, Mountain View, CA, USA) using calcium phosphate precipitation at 16-21 days *in vitro* (DIV). The neurons were fixed and analyzed within 24 hours after the transfection.

Image acquisition and spine quantification in primary hippocampal cultures

Photomicrographs were obtained using an Olympus DSU IX-81 inverted microscope fitted with a spinning disk confocal attachment and a 60x/1.2 N.A. water immersion objective. EGFP labeled neurons were chosen randomly for imaging from neuronal cultures from three coverslips. For all dendritic spine analyses, the region of the apical dendrites after the first

branch point was selected (secondary dendrite). Dendritic spine density was scored from three randomly chosen areas per neuron. Z-sections were taken at 0.3-μm intervals and were stacked with maximum projection. All analyses were conducted blind to genotype. Data were expressed as means ± SEM from independent replicates.

Spine quantitative analysis in fixed tissue

Animals were anesthetized with chloral hydrate (0.1 ml of a 15% solution, i.p.), and perfused transcardially with ice-cold 1% paraformaldehyde in 0.1 M phosphate-buffered saline (PBS, pH 7.4) for 1 minute followed by 4% paraformaldehyde in 0.1 M PBS with 0.125% glutaraldehyde for 12 minutes. The brains were carefully removed from the skull and postfixed overnight at 4°C in 4% paraformaldehyde in PBS with 0.125% glutaraldehyde. The brains were then transferred to PBS, sectioned at 200 μm on a Vibratome (Leica VT1000S, Bannockburn, IL, USA), and stored at 4°C in PBS until ready for use.

Intracellular dye injections

For intracellular injections, sections were incubated in 4′,6-diamidino-2-phenylindole (DAPI; Sigma, St. Louis, MO, USA) for 5 minutes to reveal the cytoarchitectural features of the pyramidal layer of CA1 of the hippocampus. The sections were then mounted on nitrocellulose paper and immersed in ice-cold 0.1 M PBS. Pyramidal neurons in the CA1 region were injected with an intracellular iontophoretic injection of 5% Lucifer Yellow (Molecular Probes, Eugene, OR, USA) in PBS under a DC current of 3-8 nA for 3-5 minutes, or until the dye had completely filled distal processes and no further loading was observed (Duan et al., 2002; Duan et al., 2003; Hao et al., 2006; Radley et al., 2006; Radley et al., 2008). Five to 10 neurons were injected per slice and placed far enough apart to minimize overlap of their dendritic trees. Brain sections containing loaded neurons were then mounted on slide in Fluoromount G (Beckman Coulter, Fullerton, CA, USA).

Neuronal and dendritic reconstruction

In order for a loaded neuron to be included in the analysis, it had to satisfy the following criteria: (1) lie within the pyramidal layer of the CA1 as defined by cytoarchitectural characteristics; (2) demonstrate complete filling of dendritic tree, as evidenced by well-defined endings; (3) demonstrate intact primary and secondary branches; (4) demonstrate intact tertiary branches, with the exception of branches that extended beyond 50 μm in radial distance from the cell soma (Duan et al., 2002; Duan et al., 2003; Radley et al., 2006). Neurons meeting these criteria were reconstructed in 3-dimension (3D) with a 63x/1.4 N.A., Plan-Apochromat oil immersion objective on a Zeiss Axiophot 2 microscope equipped with a motorized stage, video camera system, and Neurolucida morphometry software (MBF Bioscience, Williston, VT, USA). Using NeuroExplorer software (MBF Bioscience), total dendritic length, number of intersections and the amount of dendritic material per radial distance from the soma, in 30-μm increments (Sholl, 1953) were analyzed in order to assess morphological cellular diversity and potential differences among animal groups.

Confocal microscopy and spine acquisition

Using an approach that minimizes sampling bias of spines, dendritic segments (20 - 25 μm in length) were selected with a systematic-random design (Duan et al., 2003; Hao et al., 2006; Radley et al., 2006) and imaged essentially as described on a Zeiss LSM 510 confocal microscope (Zeiss, Thornwood, NY, USA) using a 100X/1.4 N.A. Plan-Apochromat objective with a digital zoom of 3.5 and an Ar/Kr laser at an excitation wavelength of 488 nm. All confocal stacks were acquired at 512 × 512 pixel resolution with a z-step of 0.1 μm. All confocal stacks included approximately 1 μm above and below the identified dendritic

segment. On average, three z-stacks were imaged per neuron. In order for a dendritic segment to be optically imaged, it had to satisfy the following criteria: (1) the entire segment had to fall within a depth of 50 μm; (2) dendritic segments had to be either parallel or at acute angles to the coronal surface of the section; and (3) segments did not overlap other segments that would obscure visualization of spines (Radley et al., 2006; Radley et al., 2008). Confocal stacks were then deconvolved using an iterative blind deconvolution algorithm (AutoDeblur version 8.0.2; MediaCybernetics, Bethesda, MD, USA). This step is necessary because in the raw image, the image spread in the z-plane would limit the precise interpretation of 3D spine morphology.

Spine analysis

After deconvolution, confocal stacks were analyzed with NeuronStudio (Rodriguez et al., 2008; Rodriguez et al., 2006; Wearne et al., 2005) (http://www.mssm.edu/cnic) to examine global and local morphometric characteristics of dendrites and spines such as dendritic spine densities, dendritic spine shape (stubby, mushroom, and thin), and dendritic spine volume. This software allows for automated digitization and reconstructions of 3D neuronal morphology from multiple confocal stacks on a spatial scale and averts the subjective errors encountered during manual tracing using a Rayburst-based spine analysis (Rodriguez et al., 2008; Rodriguez et al., 2006). At least three dendritic segments per apical dendrite were analyzed per cell with each segment manually inspected and appropriate corrections made using the NeuronStudio interface. Five neurons were analyzed from each animal and 5 mice were examined from each genotype in both age groups.

sAPP construct and sAPP transfection

sAPPα and sAPPβ construct were created by introducing the stop codon immediately following the α-secretase cleavage site (HQK^LV) or β-secreatase cleavage site (VKM^DAE) to mouse APP 695 pcDNA (sAPPΔ). The full-length mouse and sAPPΔ cDNAs were subcloned into pLNCX2 vector (Clontech) and stably transfected into rat B103 neuroblastoma cells with Lipofectamine 2000 according to the manufacturer's instructions. Following selection for G418 resistance, the cells were pooled and assayed without clonal selection. Levels of sAPP secreted into the medium were measured by Western blotting with rabbit polyclonal antibody 63G which recognizes the extracellular domain of APP (Marquez-Sterling et al., 1997). Rabbit polyclonal antibody CT15 that recognizes the C-terminus of APP was used to verify full-length protein in cell lysates (Soriano et al., 2001). Transfected B103 cells were cultured in DMEM plus 10% fetal calf serum but switched to neurobasal medium with B-27 supplement overnight for conditioning and the medium was harvested and stored at −80 °C until use.

Acute hippocampal slice electrophysiology

Acute horizontal hippocampal slices were made from 2-4 months- and 12 months-old from APP−/− mice and their control littermates (APP+/−). Following euthanasia with isoflurane, 400 μm-thick hippocampal slices were cut with a vibroslicer (Campden Instruments, Leicester, UK). The brain slices were kept at room temperature for 1-2 hours before transfer to a recording chamber in artificial CSF (ACSF) containing (in mM) 125 NaCl, 2.4 KCl, 1.2 NaH_2PO_4, 1 $CaCl_2$, 2 $MgCl_2$, 25 $NaHCO_3$, and 25 glucose. In the recording chamber, the slices were perfused with oxygenated ASCF containing 2 mM $CaCl_2$ and 1 mM $MgCl_2$. Extracellular recordings of excitatory postsynaptic potentials (fEPSPs) were obtained from the stratum radiatum in the CA1 area using microelectrodes filled with extracellular recording solution. A bipolar stimulating electrode was placed in the stratum radiatum for stimulation of the Schaffer collateral/commissural pathway. Basal synaptic transmission was assessed by comparing the input and output relationship of the fEPSPs recorded. For each animal, we measured the fiber volley amplitude and initial slope of the fEPSP responses to a

range of stimulation from 100 to 900 μA, and the stimulus intensity was adjusted individually for each experiment to produce fEPSPs, which are 30-40% of the maximal responses (submaximal) that could be evoked. The strength of synaptic transmission was quantified by measuring the amplitude of the peak amplitude of the fiber volley (input) and the initial slope of the fEPSP (output). The basal synaptic transmission was assessed by the input–output curve (I/O). The I/O curve was plotting all individual fEPSP slope and fiber volley values and fit data by linear regression analysis. The short-term and long-term synaptic modification will be measured by pair-pulse facilitation (PPF) and long-term potentiation (LTP), respectively. PPF will be evoked with interstimulus intervals of 50 ms at submaximal stimulus intensities. PPF is expressed as the ratio of the peak amplitude of fEPSP (second stimulation) / fEPSP (first stimulation). LTP will be induced by four tetani delivered 20 s apart, each at 100 Hz for 1 s after a 20 minutes baseline period. fEPSPs were monitored for 60 minutes after tetanus. The raw data was collected and analyzed by using pClamp 10 software (Molecular Devices, Sunnyvale, CA, USA).

Western blotting

Briefly, the brain tissue was homogenized in CHAPSO and proteinase inhibitor (Sigma-Aldrich). The homogenate was centrifuged at 100,000 *g* for 1 hour. Protein concentrations from each sample were measured by BCA method (Pierce Biotechnology Inc., Rockford, IL, USA). The rabbit polyclonal anti-PSD-95 antiserum was purchased from Biosource Inc., (Camarillo, CA, USA), and the monoclonal anti-synaptophysin antibody was purchased from Millipore (Temecula, CA, USA). The anti-β-tubulin antibody E7-a1 was obtained from the Developmental Studies Hybridoma Bank.

Statistical analysis

For *in vitro* studies in primary hippocampal neurons, all experiments were repeated 3 to 5 times. The spine density was compared by one-way ANOVA with Tukey's post-hoc test when compared between-genotypes and different treatment. The unpaired *t*-test was used as compared the two treatments within the same genotype of neurons. For the *in vivo* studies, values for each APP−/− animal and their APP+/− counterparts were obtained by taking the average of the data from all neurons for each animal. An independent sample *t*-test was performed on spine density, spine percentage, spine volume, and dendritic length. Sholl analysis data were compared by repeated measures ANOVA with Bonferroni post-hoc test with genotype (APP−/− *vs.* APP+/−) as the between-group factor and distance from the soma as the repeated-measures factor (Dickstein et al., 2010; Radley et al., 2008). The α level was set at 0.05 for all analyses in the study, and all data were represented as mean ± SEM. All statistical analyses were carried out using Prism software (GraphPad Software, Inc, La Jolla, CA, USA).

Supplementary Material

Refer to Web version on PubMed Central for supplementary material.

Acknowledgments

The authors would like to acknowledge support from the following NIH grants P50 AG05138 (DLD, PRH) and R01 AG032179 (EHK), AHAF grant A2010361 (SHT), and the microscopy facility at UCSD Specialized Cancer Center, Support Grant P30 CA23100.

Abbreviations

AD Alzheimer's disease

APP	amyloid precursor protein
eGFP	enhanced green fluorescent protein
LTP	long-term potentiation
PPF	paired-pulse facilitation
CM	conditioned medium
PBS	phosphate-buffered saline
fEPSP	excitatory postsynaptic potentials
Aβ	amyloid β-protein
CTFs	C-terminal fragments
AICD	APP intracellular domain
KO	knock-out
DIV	days in vitro

References

Alvarez VA, Sabatini BL. Anatomical and physiological plasticity of dendritic spines. Annu Rev Neurosci. 2007; 30:79–97. [PubMed: 17280523]

Anliker B, Muller U. The functions of mammalian amyloid precursor protein and related amyloid precursor-like proteins. Neurodegener Dis. 2006; 3:239–246. [PubMed: 17047363]

Barbagallo AP, Wang Z, Zheng H, D'Adamio L. A single tyrosine residue in the amyloid precursor protein intracellular domain is essential for developmental function. J Biol Chem. 2011; 286:8717–8721. [PubMed: 21266574]

Bittner T, Fuhrmann M, Burgold S, Jung CK, Volbracht C, Steiner H, Mitteregger G, Kretzschmar HA, Haass C, Herms J. Gamma-secretase inhibition reduces spine density in vivo via an amyloid precursor protein-dependent pathway. J Neurosci. 2009; 29:10405–10409. [PubMed: 19692615]

Calabrese B, Shaked GM, Tabarean IV, Braga J, Koo EH, Halpain S. Rapid, concurrent alterations in pre- and postsynaptic structure induced by naturally-secreted amyloid-beta protein. Mol Cell Neurosci. 2007; 35:183–193. [PubMed: 17368908]

De Strooper B, Annaert W. Proteolytic processing and cell biological functions of the amyloid precursor protein. J Cell Sci. 2000; 113(Pt 11):1857–1870. [PubMed: 10806097]

Dickstein DL, Brautigam H, Stockton SD Jr. Schmeidler J, Hof PR. Changes in dendritic complexity and spine morphology in transgenic mice expressing human wild-type tau. Brain Struct Funct. 2010; 214:161–179. [PubMed: 20213269]

Duan H, Wearne SL, Morrison JH, Hof PR. Quantitative analysis of the dendritic morphology of corticocortical projection neurons in the macaque monkey association cortex. Neuroscience. 2002; 114:349–359. [PubMed: 12204204]

Duan H, Wearne SL, Rocher AB, Macedo A, Morrison JH, Hof PR. Age-related dendritic and spine changes in corticocortically projecting neurons in macaque monkeys. Cereb Cortex. 2003; 13:950–961. [PubMed: 12902394]

Epstein CJ. The consequences of chromosome imbalance. Am J Med Genet Suppl. 1990; 7:31–37. [PubMed: 2149968]

Friedland DR, Los JG, Ryugo DK. A modified Golgi staining protocol for use in the human brain stem and cerebellum. J Neurosci Methods. 2006; 150:90–95. [PubMed: 16081162]

Guo Q, Wang Z, Li H, Wiese M, Zheng H. APP physiological and pathophysiological functions: insights from animal models. Cell Res. 2011

Hao J, Rapp PR, Leffler AE, Leffler SR, Janssen WG, Lou W, McKay H, Roberts JA, Wearne SL, Hof PR, Morrison JH. Estrogen alters spine number and morphology in prefrontal cortex of aged female rhesus monkeys. J Neurosci. 2006; 26:2571–2578. [PubMed: 16510735]

Hardy J, Selkoe DJ. The amyloid hypothesis of Alzheimer's disease: progress and problems on the road to therapeutics. Science. 2002; 297:353–356. [PubMed: 12130773]

Harper SJ, Bilsland JG, Shearman MS, Zheng H, Van der Ploeg L, Sirinathsinghji DJ. Mouse cortical neurones lacking APP show normal neurite outgrowth and survival responses in vitro. Neuroreport. 1998; 9:3053–3058. [PubMed: 9804315]

Herard AS, Besret L, Dubois A, Dauguet J, Delzescaux T, Hantraye P, Bonvento G, Moya KL. siRNA targeted against amyloid precursor protein impairs synaptic activity in vivo. Neurobiol Aging. 2006; 27:1740–1750. [PubMed: 16337035]

Hoe HS, Fu Z, Makarova A, Lee JY, Lu C, Feng L, Pajoohesh-Ganji A, Matsuoka Y, Hyman BT, Ehlers MD, Vicini S, Pak DT, Rebeck GW. The effects of amyloid precursor protein on postsynaptic composition and activity. J Biol Chem. 2009; 284:8495–8506. [PubMed: 19164281]

Holcomb L, Gordon MN, McGowan E, Yu X, Benkovic S, Jantzen P, Wright K, Saad I, Mueller R, Morgan D, Sanders S, Zehr C, O'Campo K, Hardy J, Prada CM, Eckman C, Younkin S, Hsiao K, Duff K. Accelerated Alzheimer-type phenotype in transgenic mice carrying both mutant amyloid precursor protein and presenilin 1 transgenes. Nat Med. 1998; 4:97–100. [PubMed: 9427614]

Konietzko U. AICD Nuclear Signaling and its Possible Contribution to Alzheimer's Disease. Curr Alzheimer Res. 2011

Lee KJ, Moussa CE, Lee Y, Sung Y, Howell BW, Turner RS, Pak DT, Hoe HS. Beta amyloid-independent role of amyloid precursor protein in generation and maintenance of dendritic spines. Neuroscience. 2010; 169:344–356. [PubMed: 20451588]

Li H, Wang B, Wang Z, Guo Q, Tabuchi K, Hammer RE, Sudhof TC, Zheng H. Soluble amyloid precursor protein (APP) regulates transthyretin and Klotho gene expression without rescuing the essential function of APP. Proc Natl Acad Sci U S A. 2010; 107:17362–17367. [PubMed: 20855613]

Marquez-Sterling NR, Lo AC, Sisodia SS, Koo EH. Trafficking of cell-surface beta-amyloid precursor protein: evidence that a sorting intermediate participates in synaptic vesicle recycling. J Neurosci. 1997; 17:140–151. [PubMed: 8987743]

Mattson MP. Free radicals and disruption of neuronal ion homeostasis in AD: a role for amyloid beta-peptide? Neurobiol Aging. 1995; 16:679–682. discussion 683. [PubMed: 8544920]

Mattson MP. Cellular actions of beta-amyloid precursor protein and its soluble and fibrillogenic derivatives. Physiol Rev. 1997; 77:1081–1132. [PubMed: 9354812]

Midthune B, Tyan SH, Walsh JJ, Sarsoza F, Eggert S, Hof PR, Dickstein DL, Koo EH. Deletion of the amyloid precursor-like protein 2 (APLP2) does not affect hippocampal neuron morphology or function. Mol Cell Neurosci. 2012; 49:448–455. [PubMed: 22353605]

Nunan J, Shearman MS, Checler F, Cappai R, Evin G, Beyreuther K, Masters CL, Small DH. The C-terminal fragment of the Alzheimer's disease amyloid protein precursor is degraded by a proteasome-dependent mechanism distinct from gamma-secretase. Eur J Biochem. 2001; 268:5329–5336. [PubMed: 11606195]

Phinney AL, Calhoun ME, Wolfer DP, Lipp HP, Zheng H, Jucker M. No hippocampal neuron or synaptic bouton loss in learning-impaired aged beta-amyloid precursor protein-null mice. Neuroscience. 1999; 90:1207–1216. [PubMed: 10338291]

Pilati N, Barker M, Panteleimonitis S, Donga R, Hamann M. A rapid method combining Golgi and Nissl staining to study neuronal morphology and cytoarchitecture. J Histochem Cytochem. 2008; 56:539–550. [PubMed: 18285350]

Potter H. Review and hypothesis: Alzheimer disease and Down syndrome--chromosome 21 nondisjunction may underlie both disorders. Am J Hum Genet. 1991; 48:1192–1200. [PubMed: 1827946]

Priller C, Bauer T, Mitteregger G, Krebs B, Kretzschmar HA, Herms J. Synapse formation and function is modulated by the amyloid precursor protein. J Neurosci. 2006; 26:7212–7221. [PubMed: 16822978]

Radley JJ, Rocher AB, Miller M, Janssen WG, Liston C, Hof PR, McEwen BS, Morrison JH. Repeated stress induces dendritic spine loss in the rat medial prefrontal cortex. Cereb Cortex. 2006; 16:313–320. [PubMed: 15901656]

Radley JJ, Rocher AB, Rodriguez A, Ehlenberger DB, Dammann M, McEwen BS, Morrison JH, Wearne SL, Hof PR. Repeated stress alters dendritic spine morphology in the rat medial prefrontal cortex. J Comp Neurol. 2008; 507:1141–1150. [PubMed: 18157834]

Ring S, Weyer SW, Kilian SB, Waldron E, Pietrzik CU, Filippov MA, Herms J, Buchholz C, Eckman CB, Korte M, Wolfer DP, Muller UC. The secreted beta-amyloid precursor protein ectodomain APPs alpha is sufficient to rescue the anatomical, behavioral, and electrophysiological abnormalities of APP-deficient mice. J Neurosci. 2007; 27:7817–7826. [PubMed: 17634375]

Rodriguez A, Ehlenberger DB, Dickstein DL, Hof PR, Wearne SL. Automated three-dimensional detection and shape classification of dendritic spines from fluorescence microscopy images. PLoS One. 2008; 3:e1997. [PubMed: 18431482]

Rodriguez A, Ehlenberger DB, Hof PR, Wearne SL. Rayburst sampling, an algorithm for automated three-dimensional shape analysis from laser scanning microscopy images. Nat Protoc. 2006; 1:2152–2161. [PubMed: 17487207]

Russo T, Faraonio R, Minopoli G, De Candia P, De Renzis S, Zambrano N. Fe65 and the protein network centered around the cytosolic domain of the Alzheimer's beta-amyloid precursor protein. FEBS Lett. 1998; 434:1–7. [PubMed: 9738440]

Schubert D, Behl C. The expression of amyloid beta protein precursor protects nerve cells from beta-amyloid and glutamate toxicity and alters their interaction with the extracellular matrix. Brain Res. 1993; 629:275–282. [PubMed: 7906601]

Seabrook GR, Smith DW, Bowery BJ, Easter A, Reynolds T, Fitzjohn SM, Morton RA, Zheng H, Dawson GR, Sirinathsinghji DJ, Davies CH, Collingridge GL, Hill RG. Mechanisms contributing to the deficits in hippocampal synaptic plasticity in mice lacking amyloid precursor protein. Neuropharmacology. 1999; 38:349–359. [PubMed: 10219973]

Sholl DA. Dendritic organization in the neurons of the visual and motor cortices of the cat. J Anat. 1953; 87:387–406. [PubMed: 13117757]

Sisodia SS, Koo EH, Hoffman PN, Perry G, Price DL. Identification and transport of full-length amyloid precursor proteins in rat peripheral nervous system. J Neurosci. 1993; 13:3136–3142. [PubMed: 8331390]

Soriano S, Lu DC, Chandra S, Pietrzik CU, Koo EH. The amyloidogenic pathway of amyloid precursor protein (APP) is independent of its cleavage by caspases. J Biol Chem. 2001; 276:29045–29050. [PubMed: 11397796]

Turner PR, O'Connor K, Tate WP, Abraham WC. Roles of amyloid precursor protein and its fragments in regulating neural activity, plasticity and memory. Prog Neurobiol. 2003; 70:1–32. [PubMed: 12927332]

Wang P, Yang G, Mosier DR, Chang P, Zaidi T, Gong YD, Zhao NM, Dominguez B, Lee KF, Gan WB, Zheng H. Defective neuromuscular synapses in mice lacking amyloid precursor protein (APP) and APP-Like protein 2. J Neurosci. 2005; 25:1219–1225. [PubMed: 15689559]

Wearne SL, Rodriguez A, Ehlenberger DB, Rocher AB, Henderson SC, Hof PR. New techniques for imaging, digitization and analysis of three-dimensional neural morphology on multiple scales. Neuroscience. 2005; 136:661–680. [PubMed: 16344143]

Weyer SW, Klevanski M, Delekate A, Voikar V, Aydin D, Hick M, Filippov M, Drost N, Schaller KL, Saar M, Vogt MA, Gass P, Samanta A, Jaschke A, Korte M, Wolfer DP, Caldwell JH, Muller UC. APP and APLP2 are essential at PNS and CNS synapses for transmission, spatial learning and LTP. Embo J. 2011; 30:2266–2280. [PubMed: 21522131]

Zheng H, Jiang M, Trumbauer ME, Sirinathsinghji DJ, Hopkins R, Smith DW, Heavens RP, Dawson GR, Boyce S, Conner MW, Stevens KA, Slunt HH, Sisoda SS, Chen HY, Van der Ploeg LH. beta-Amyloid precursor protein-deficient mice show reactive gliosis and decreased locomotor activity. Cell. 1995; 81:525–531. [PubMed: 7758106]

Zheng H, Koo EH. Biology and pathophysiology of the amyloid precursor protein. Mol Neurodegener. 2011; 6:27. [PubMed: 21527012]

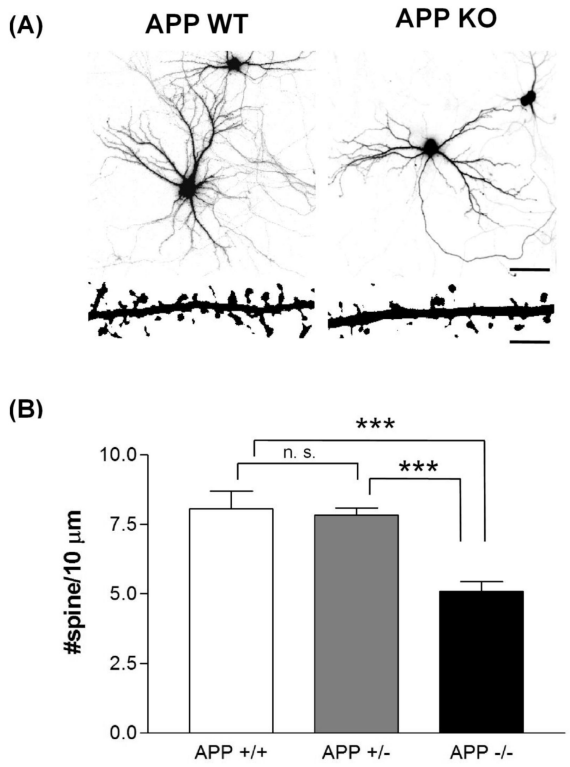

Figure 1.

APP−/− hippocampal neurons show a decrease in spine number. (A) Representative images of primary hippocampal neurons expressing eGFP. Top: APP+/− (left) and APP−/− (Holcomb et al., 1998) neurons were from the same parental interbreeding of APP mice. The images were presented in grey and inverted color. Panels at the bottom of each image show high-magnification renderings of dendritic segments. The dendritic images were taken with 0.3-μm step z-section and then stacked with maximum projection. Scale bar: 150 μm (top) and 5 μm (bottom). (B) Quantification of spine density. There was no difference in spine number between APP+/+ and APP+/− ($p > 0.05$). APP−/− neurons showed highly significant decrease in spine density compared to APP+/+ or APP+/− neurons (**, $p < 0.01$ and ***, $p < 0.001$). Data are expressed as mean ± SEM and tested using a one-way ANOVA with Tukey's post-hoc test.

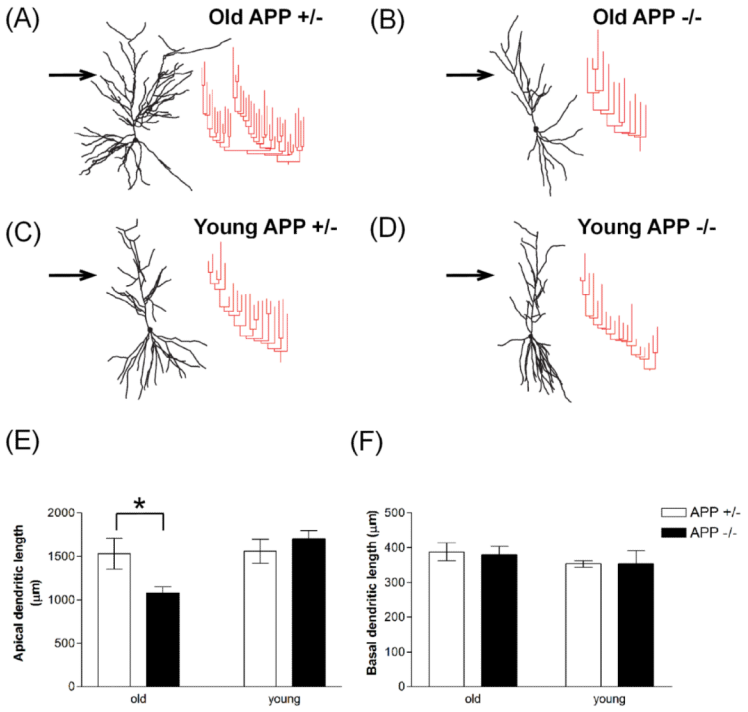

Figure 2.

3-Dimensional reconstructions of CA1 neurons. (A-D) Representative examples of 3-dimensional reconstructions of neurons and the corresponding apical dendrograms (arrow indicates the apical dendrite). Dendrograms of CA1 pyramidal layer neurons in 13 months old APP+/− and APP−/− mice (A and B); and in young APP+/− and APP−/− mice (C and D; 2-4 months old). (E) and (F) Dendrogram and quantification of dendritic length of CA1 neurons in APP−/− mice. Thirteen month-old APP−/− exhibited a significant decrease in apical length compared to APP+/−, whereas young APP−/− mice showed no significant difference in apical dendritic length compared to APP+/− mice (E). There is no difference in basal dendritic length among APP+/− and APP−/− mice of both age groups (F). Data are expressed as mean ± SEM; asterisks indicate significant differences between groups (*, $p < 0.05$; unpaired *t*-test).

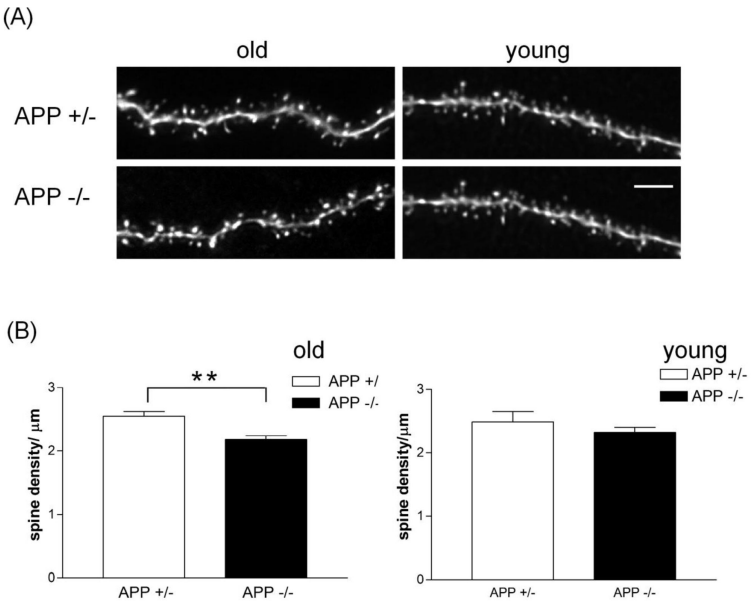

Figure 3.

Quantification of spine density in APP animal. (A) Representative dendrite images after 3-dimensional deconvolution and processing with NeuronStudio software (see methods). Scale bars: 5 μm. (B) The spine density was decreased (left) ~15% in old APP−/− mice compared to their littermate controls (APP+/−). Young APP−/− mice showed no significant difference in spine density compared to APP+/− mice. The young mice were 2-4 months old. Data are expressed as means ± SEM; asterisks indicate significant differences between groups (**, $p < 0.01$; unpaired *t*-test).

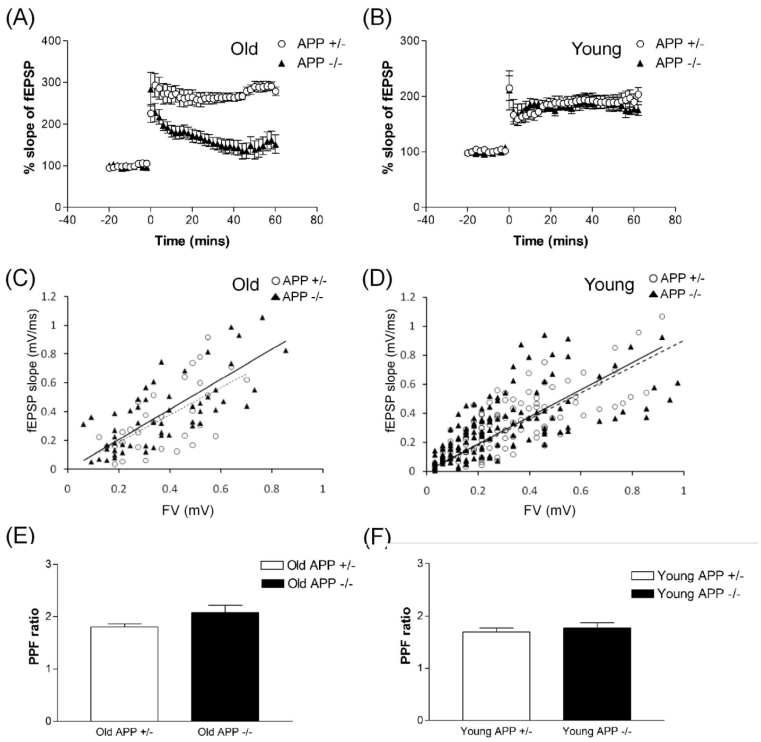

Figure 4.

APP−/− mice showed impaired electrical properties in acute hippocampal slices of old APP −/− mice. (A) 12-15 months old APP−/− mice (closed triangles) showed impairment in LTP but not in APP+/− mice (open circle). (B) Young APP−/− mice showed normal LTP as did their littermate controls. fEPSPs were recorded in stratum radiatum (dendritic area) of the CA1 region following stimulation of the Schaffer collateral pathway. LTP were induced with 4 tetanus stimulation delivered at 20-s intervals, each at 100 Hz for 1 s. (C) and (D) Basal synaptic transmission was assayed by measuring fEPSPs within the stratum radiatum of the CA1 region of the hippocampus evoked by a bipolar electrode placed at the CA3–CA1 border. For each level of stimulation, the maximum amplitude of the presynaptic fiber volley (FV; arrow) and the initial slope of the fEPSP were measured (see also supplemental Fig. 1). Scatter plot of the fEPSP slope versus fiber volley of every recording in old APP−/− mice (closed triangles, black line; n = 24 slices, 9 animals) and APP+/− mice (16 slices, 7 animals; open circle, dash line), fit by linear regression. There is no significant difference in basal transmission among APP+/− and APP−/− mice in both age groups. (E) and (F) Paired-pulse facilitation at the Schaffer collateral CA1 synapse was measured by dividing the amplitude of the second fEPSP by the amplitude of the first elicited by a pair of two 50-ms spaced stimuli. No significant change in PPF ratio was observed in both age groups between APP+/− and APP−/− mice.

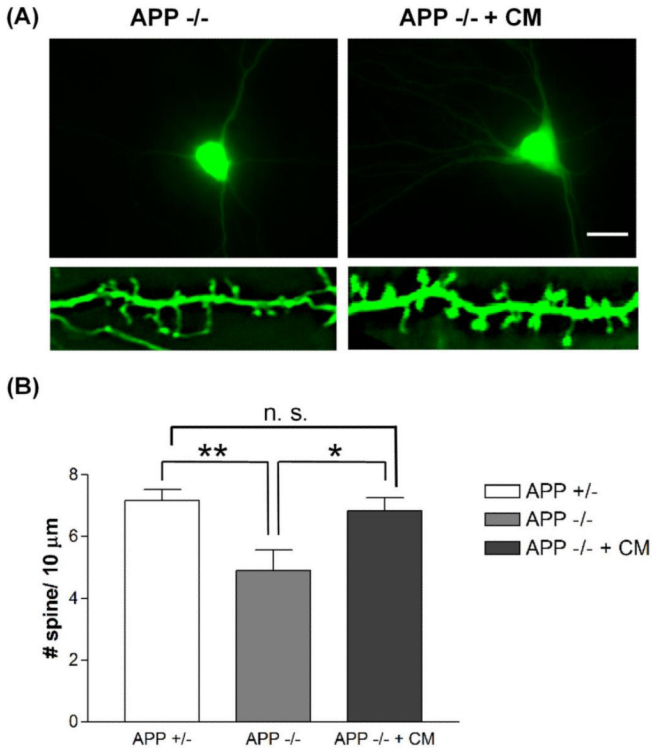

Figure 5.

APP deficient effects on spines are prevented by adding conditioned medium (CM) from APP wild type neurons (APP+/+ or APP+/−). (A) Representative culture APP−/− hippocampal neurons expressing eGFP: APP−/− neurons are shown at right and wild type CM-treated APP−/− neurons at left. Scale bars: 20 (top) and 5 (bottom) μm. Wild type CM was replaced with medium on the second day after plating the neurons. The medium was changed every other day. The bottom of each image shows high-magnification micrographs of dendrites. (B) The quantification of spine density. Wild types CM rescue the decrease in spine density of APP−/− neurons (*, $p < 0.05$; **, $p < 0.01$, unpaired *t*-test).

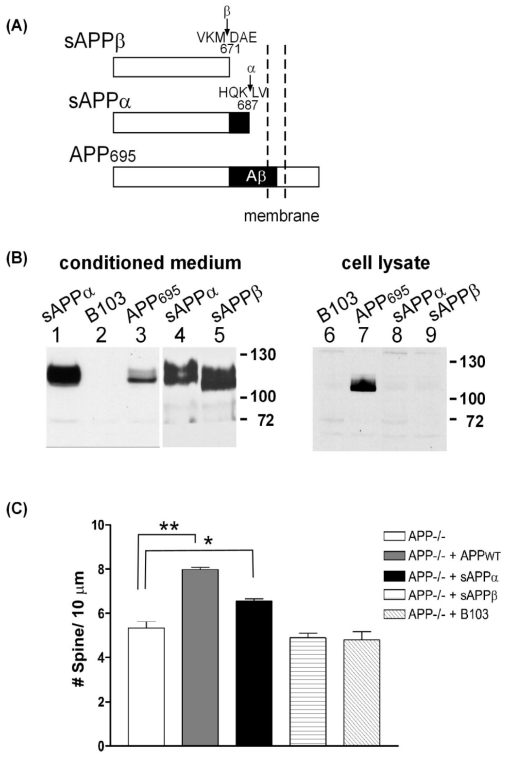

Figure 6.

Soluble APPα but not soluble APPβ rescued partially deficits in dendritic spine number and morphology. (A) The scheme of soluble mouse APP (sAPPα and sAPPβ) and full length of mouse APP (APP). (B) left, 63G antibody (the polyclonal antibody against the middle region of APP) Western blot from medium of B103 cells transfected with either sAPPα (lanes 1 and 4 from two of single clone), sAPPβ (lane 5) or mouse APP695 (APP) constructs (lane 3) and the non-transfected control (lane 2); Right: CT15 immunoblot from cell lysates of untransfected (lane 6), mouse APP-transfected (lane 7), sAPPα-transfected (lane 8) and sAPPβ-transfected B103 cells (lane 9). (c) Quantification of spine density. APP −/− neurons were treated with medium from either sAPPα-, sAPPβ- and vehicle-transfected B103 cells or from the conditioned medium of APP WT (APP+/+ or APP+/−) neurons (each treatment is indicated in the bar legend). The spine density was restored partially in sAPPα-treated APP−/− neurons compared to APP−/− neurons (*, $p < 0.05$, unpaired *t*-test). The sAPPβ-CM did not restore spine density in APP−/− neurons ($p > 0.5$, unpaired *t*-test).

Table 1

Dendrite and spine morphometry from CA1 pyramidal neurons from APP+/− and APP−/− aged and young mice.

Age	Genotype	Morphology (μm)		Spine						
				Density (spines/μm)	Type (%)			Volume (μm3)		
		Apical	Basal	Apical	Apical			Apical		
					S	T	M	S	T	M
Young	APP+/−	1561.32 ± 140.71	353.8 ± 9.35	2.49 ± 0.17	36.26 ± 1.87	53.20 ± 1.21	10.55 ± 0.96	0.045 ± 0.002	0.034 ± 0.002	0.155 ± 0.014
	APP−/−	1706.37 ± 95.31	353.9 ± 37.57	2.32 ± 0.08	39.02 ± 1.75	49.13 ± 1.73	11.85 ± 0.71	0.045 ± 0.001	0.03 ± 0.002	0.138 ± 0.001
Aged	APP+/−	*1534.7 ± 178.7	388.6 ± 25.72	2.50 ± 0.05	44.19 ± 1.26	44.01 ± 1.47	11.98 ± 0.97	0.052 ± 0.002	0.036 ± 0.001	0.148 ± 0.009
	APP−/−	*1084.3 ± 68.95	380.4 ± 23.86	2.16 ± 0.05**	45.29 ± 3.01	41.52 ± 0.96	13.18 ± 2.41	0.052 ± 0.002	0.036 ± 0.001	0.148 ± 0.009

S stubby spine, T thin spine, M mushroom spine.

* $p < 0.05$;

** $p < 0.01$.